

Polarized-photon—scattered-particle correlation measurements in $H^+ + He$ collisions

D. W. Mueller* and D. H. Jaecks

Behlen Laboratory of Physics, University of Nebraska, Lincoln, Nebraska 68588

(Received 13 May 1985)

Measurements of the relative magnetic-substate population of differentially scattered $H(2p)$ atoms formed in 4-, 5-, and 8-keV proton-helium collisions have been made using polarized-photon—scattered-particle coincidence techniques. The relative phases of the scattering amplitudes were also determined. It was found that the differential cross sections for the magnetic substates $m_l=0$ and $m_l=\pm 1$ were of comparable magnitude indicating that translational and rotational coupling play equally important roles in the excitation process. The average measured phase difference was found to be $|45^\circ|$.

I. INTRODUCTION

Using polarized-photon correlation measurement techniques one can often determine relative populations of magnetic substates and the relative phases of the scattering amplitudes.¹ Within the context of the molecular-orbital (MO) model² of ion-atom collisions, this information takes on added significance because there is a one-to-one correspondence between the molecular-orbital quantum numbers of the collision complex and the separated-atom quantum numbers. One role of experiment is to delineate the excitation mechanisms of these MO states and test the range of validity of the model.

Most inelastic processes in ion-atom systems studied to date are dominated by crossings of the initial-state molecular orbitals with those leading to the final state.³ These crossings occur from internuclear separations of several

atomic units down to the united-atom limit.

The $H^+ + He$ collision system is of particular interest because the excitation process is dominated by mechanisms involving large internal energy changes within the temporal molecule rather than by curve crossing. This feature of the HeH^+ system is illustrated in the diabatic molecular-orbital correlation diagram in Fig. 1: the initial $(1s\sigma)^2$ configuration is separated by about 10 eV from the $1s\sigma 2p\sigma$ configuration that leads to the charge-transfer state of $H(1s) + He^+$.

The HeH^+ system is also important because accurate potential curves and matrix elements for the system exist⁴ and it could well serve as a two-electron prototype system where the initial state is well separated in energy from the final state.

II. EXPERIMENTAL PROCEDURE AND RESULTS

The accelerator and collision chamber for the present measurements have been described elsewhere.⁵ The important features of the experiment are shown in Fig. 2. A Brewster-angle polarizer⁶ and uv photomultiplier (PM) assembly view the interaction volume of the incident proton beam and He-target gas jet formed by a stainless-steel hypodermic needle. The polarized $L\alpha$ radiation, emitted in a direction perpendicular to the scattering plane, from the $H(2p)$ state formed in the reaction

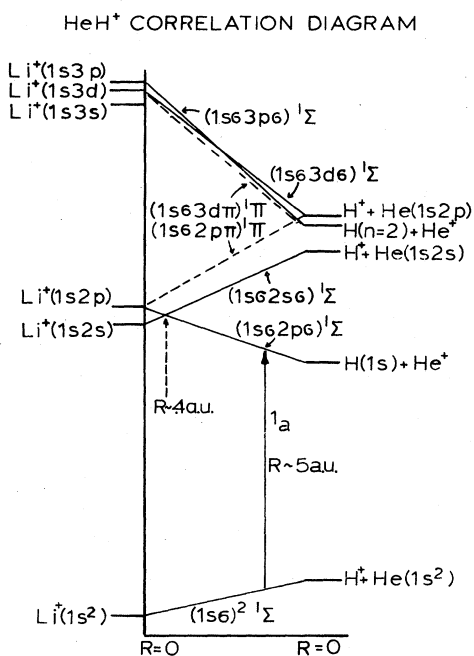
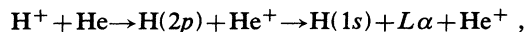


FIG. 1. HeH^+ correlation diagram.

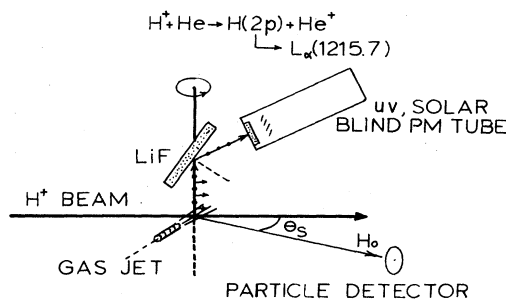


FIG. 2. Experimental arrangement for measuring the relative $L\alpha$ polarization intensity $I(\beta)$ for specific scattering angles θ_s .

is measured in coincidence with the scattered H(1s) atom for specific laboratory angles θ_s .

The total number of polarized- $L\alpha$ -photon-scattered-neutral-particle coincidences, per scattered neutral particle, was measured for four separate polarization directions, $\beta=0^\circ, 45^\circ, 90^\circ, 135^\circ$, for specific particle scattering angles θ_s . Typical measurements of the number of coincidences per scattered neutral particle, $I(\beta)$, are shown in Fig. 3 for specific scattering angles at 4-keV incident ion energy. The angle β is measured from the positive-beam axis in a clockwise direction as is θ_s .

It is important to remember that this polarization pattern is a direct image of the time-averaged electron cloud when the nuclei are far apart. This may be of particular importance when a degeneracy of the magnetic sublevels occurs allowing the electron cloud to remain fixed in space as the internuclear axis rotates.⁷⁻⁹ In this case the angle at which the electron cloud is fixed in space may be directly related to the geometrical angle formed by the impact parameter and the so-called locking distance. When no such simple interpretation exists, it may be more enlightening to discuss the pattern in the separated-atom reference frame. The measured values of $I(\beta)$ are related to the magnetic-substate cross sections, $\sigma_0(m_l=0)$ and $\sigma_1(m_l=\pm 1)$, and the relative phase χ of their scattering amplitudes a_0 and a_1 by the expression¹⁰

$$I(\beta) = c [(5\sigma_0 + 4\sigma_1) + (6\sigma_1 - 3\sigma_0)\sin^2\beta + (3\sqrt{2}\sigma_0\sigma_1\cos\chi)\sin(2\beta)], \quad (1)$$

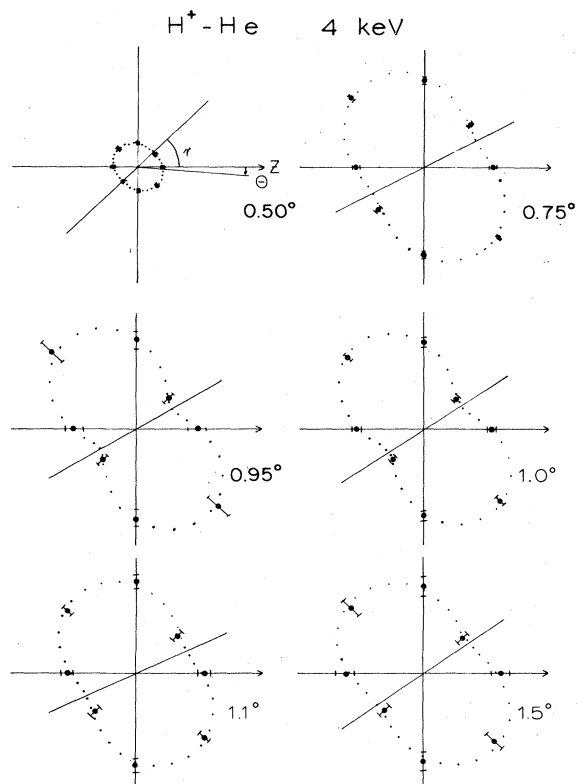


FIG. 3. Relative $L\alpha$ -polarization intensities $I(\beta)$ for H(1s) scattering angles varying from 0.5° to 1.5° at 4 keV incident ion energy.

assuming the excitation is completely coherent. A least-squares fit of the function to the measured values at $\beta=0^\circ, 45^\circ, 90^\circ$, and 135° yields the values of σ_0 , σ_1 , and χ .

As stated, the above expression for $I(\beta)$ is valid when the excitation of the H(2p) states can be described by a set of amplitudes that have fixed relative phases. Possible sources of incoherent radiation are cascading from higher n states to the H(2p) levels, excitation and formation of H(2p) from protons interacting with the background gas, and contributions from H atoms that have contaminated the primary beam. In general, cascade contributions add an incoherent contribution to the radiation. Because of the longer lifetime of the higher-lying levels and the high velocity of keV atoms, the cascade population occurs outside the valence viewed by the photon detector. Considering these effects, estimates of the cascade contributions indicate they are less than 3% of the $L\alpha$ coincidence signal. The $L\alpha$ -scattered-particle coincidence rate was measured for beam-background-gas collisions. This was found to be zero, thus eliminating this interaction as a source of incoherency. The neutral component of the primary H⁺ beam was determined by directly measuring the H-atom flux at 0° in the presence of only the ambient background gas. In this way the contribution to the H component due to charge transfer along the entire path of the beam could be determined. For 8 keV energy the H-atom component was about 10^{-5} of the H⁺ component before the target gas jet was turned on. The best check for coherency is the polarization data itself.

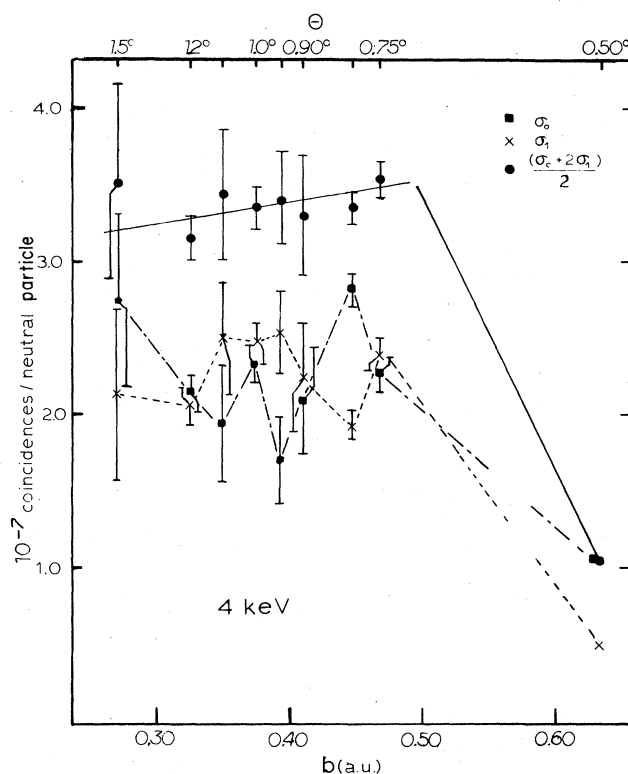


FIG. 4. Magnetic-substate cross sections σ_0 , σ_1 , and $\sigma_0+2\sigma_1$, normalized to the number of neutral particles scattered for 4 keV incident ion energy.

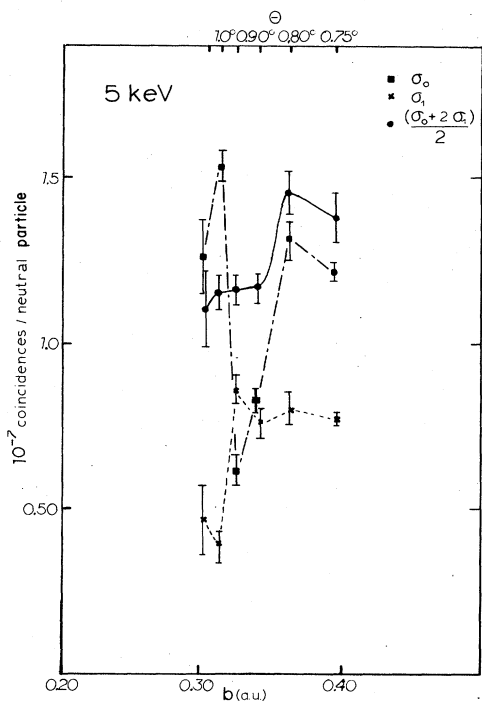


FIG. 5. Magnetic-substate cross sections σ_0 , σ_1 , and $\sigma_0 + 2\sigma_1$, normalized to the number of neutral particles scattered for 5 keV incident ion energy.

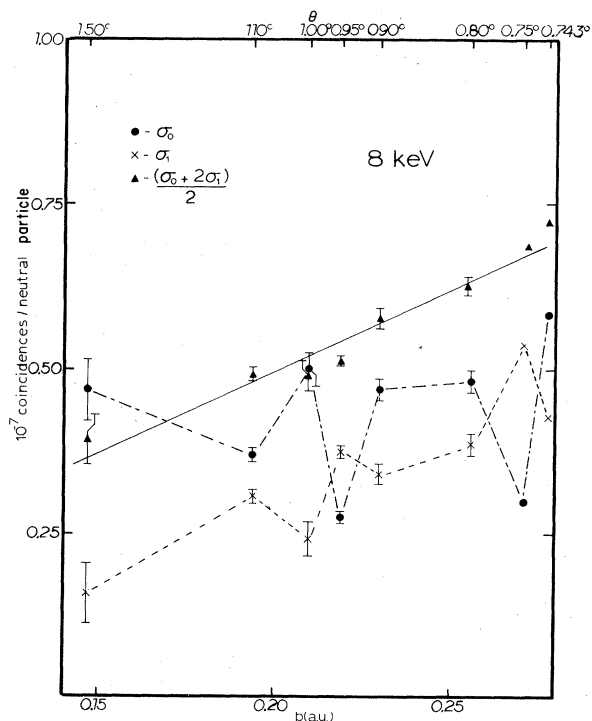


FIG. 6. Magnetic-substate cross sections σ_0 , σ_1 , and $\sigma_0 + 2\sigma_1$, normalized to the number of neutral particles scattered for 8 keV incident ion energy.

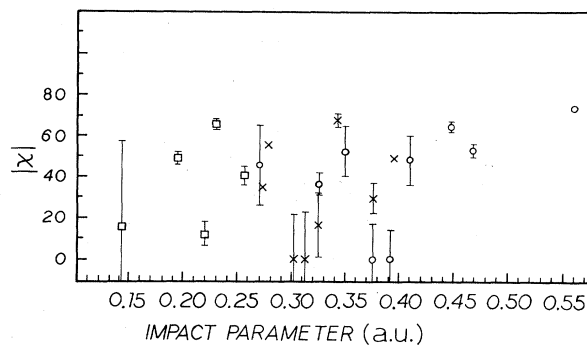


FIG. 7. Phase difference χ of the scattering amplitudes of $H(2p_0)$ and $H(2p_{\pm 1})$.

The measured values of $I(\beta)$ for 5 and 8 keV also show the general shape of the dipole pattern with the major axis always in the same approximate direction of $\beta = 60^\circ$. We note that in Fig. 3 for 0.95° and 1.0° scattering the dipole polarization pattern is characteristic of completely coherent $2p$ radiation¹⁰ suggesting that extraneous depolarizing effects such as cascade and neutral-atom contamination of the beam are not important. A major check of the consistency of the measured values of $I(\beta)$ was to perform the same measurements at negative scattering angles. Reflection symmetry through the scattering plane dictates that the measured polarization pattern for negative scattering angles should have the major axis at $\beta = -60^\circ$, which was found to be the case experimentally.

The measured relative values of σ_0 and σ_1 , normalized to the number of scattered neutral particles for 4, 5, and 8 keV, are shown in Figs. 4, 5, and 6. The data are plotted as a function of the scattering angle θ , and the impact parameter b using the results of Dose¹¹ to relate the scattering angle to an impact parameter. Also plotted in these figures are half the total cross sections to the $H(2p)$ state, $\sigma_0 + 2\sigma_1$. The magnitude of the relative phase χ is shown in Fig. 7 for 4-, 5-, and 8-keV incident ion energy.

III. DISCUSSION OF RESULTS

Knowing the measured results of σ_0 , σ_1 , and χ we are in a position to interpret the inelastic collision process $H^+ + He \rightarrow H(2p) + He^+$ in terms of the diabatic potentials of the HeH^+ as shown in Fig. 1. The population of temporal molecular Σ states should lead to $H(2p_0)$ and Π states should lead to $H(2p_{\pm 1})$ formation. The phase difference χ of the scattering amplitudes results from the different excitation mechanisms and the time development of the adiabatic phase factors from time $-\infty$ to time $+\infty$.

If we use a two-state approach to the description, that is, assume the collision takes place by a series of single transitions from one molecular state to another, transitions between two states k and n , defined in the rotating frame of the temporal molecule, are governed by the equation

$$\left\langle u_k \left| -\frac{\partial}{\partial t} \right| u_n \right\rangle = - \left\langle u_k \left| \dot{R} \frac{\partial}{\partial R} + i\omega \hat{L}_y \right| u_n \right\rangle. \quad (2)$$

Here R is the time-dependent internuclear separation and ω is the angular velocity of the internuclear axis. The term $\hat{R}\partial/\partial R$ connects states of the same symmetry, that is, Σ - Σ and Π - Π , and is generally called the radial-coupling matrix element. The second term, $i\omega\hat{L}_y$, connects states differing in electronic quantum number λ by ± 1 , that is, Σ - Π and Π - Δ , and is known generally as the rotational-coupling matrix element. The charge-transfer channel designated by $(1s\sigma 2p\sigma)^1\Sigma$ begins to be populated at an internuclear separation $R \approx 5$ a.u. (Ref. 4) as indicated by the transition labeled $1a$ in Fig. 1. Subsequent transitions to higher-lying Σ and Π states lead to the population of $H(2p_0)$ and $H(2p_{\pm 1})$.

The relative values of σ_0 and σ_1 are direct measures of the relative importance of the translational and rotational coupling terms. Our first general conclusion that we can draw from the data of Figs. 4, 5, and 6 about the inelastic mechanisms is that after the initial $(1s\sigma)^2\Sigma \rightarrow (1s\sigma 2p\sigma)\Sigma$ translational transition, rotational and translational coupling play equally important roles in the subsequent population of the $H(2p)$ state.

This differs from the results of Fayeton *et al.*,¹² where they interpreted the depopulation of the $(1s\sigma 2p\sigma)^1\Sigma$ state as being dominated by rotational coupling to the $(2s\sigma 2p\pi)^1\Pi$ state near the united-atom limit, for the process $\text{He}^+ + \text{H} \rightarrow \text{He}^+ + \text{H}(2p)$. If rotational coupling were the dominant mechanism in our case, we would observe a coincidence pattern $I(\beta)$ peaked at $\beta = 90^\circ$ with the ratio of $I(\beta = 90^\circ)/I(\beta = 0^\circ) = 2.5$.¹ From Fig. 3, we see this is clearly not the case.

A second general observation of the results for σ_0 , σ_1 , and $\sigma_0 + 2\sigma_1$, shown in Figs. 4, 5, and 6, is that σ_0 and σ_1 vary rapidly with impact parameter b , whereas the total differential cross section to the $2p$ state, $\sigma_0 + 2\sigma_1$, varies slowly. This suggests that some mechanism causes amplitude to be alternately shared between the final-state Π and Σ channels as the impact parameter is changed.

We also note that the present results are consistent with the results of McKnight and Jaecks¹³ for $H(2p)$ excitation as well as with Crandall and Jaecks¹⁴ for $H(2s)$ excitation at 6.25 keV incident ion energy. These previous results are shown in Fig. 8 and are given as probabilities as a function of impact parameter. The probability for $H(2s)$ formation is, within experimental error, constant with impact parameter. This is consistent with the present values of σ_0 at 8 keV, where the same region of impact parameter is probed. From Fig. 6, we note that σ_0 oscillates about a constant value. The earlier $H(2s)$ measurements were not sufficiently precise to observe such oscillations. The previously measured total probability for $H(2p)$ (Ref. 13) is consistent with the presently measured values of $\sigma_0 + 2\sigma_1$ plotted in Fig. 6; there is an increase in this function as the impact parameter is increased from 0.15 to 0.30 a.u.

The calculations of the rotational coupling probability performed by Taulbjerg, Briggs, and Vaaben¹⁵ for symmetrical systems are consistent with our measured value of σ_1 at 8 keV (Fig. 6). Both the calculated, shown in Fig. 9, and the measured value of σ_1 show a general increase in value as the impact parameter is increased from 0.15 to 0.5 a.u.

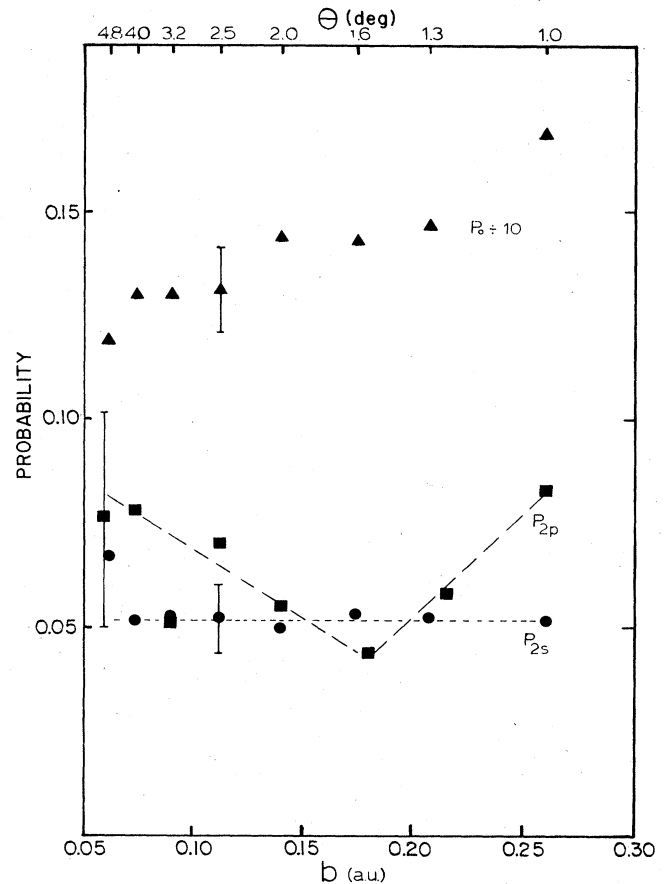


FIG. 8. Charge-transfer probabilities for $H(2s)$ and $H(2p)$ formation at 6.25 keV from Refs. 13 and 14. Total charge-transfer probability P_0 is from Ref. 14.

Another general trend to note in the data relates to the relative phase χ . From Fig. 7, we find that χ oscillates about a value of approximately $|45^\circ|$ as the impact parameter is varied. It is well known that Landau-Zener theory predicts phase changes of about 45° at avoided crossings.¹⁶⁻¹⁸ This fact prompted us to investigate the

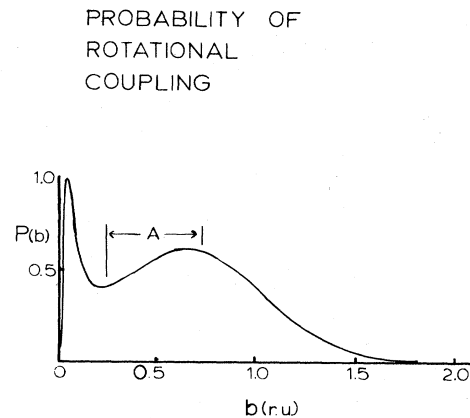


FIG. 9. Rotational coupling probability vs. impact parameter from Ref. 15. The relative units (r.u.) of Ref. 15 are taken to be equal to atomic units (a.u.) used in this text.

possibility that our observed phase differences were related to such avoided potential crossings of the HeH^+ system.

IV. PHASE CHANGES AT LANDAU-ZENER CROSSINGS

To determine the phase change of population amplitudes of diabatic crossings or avoided adiabatic crossings of potential curves, we have adopted the procedure set forth by Ankudinov, Bobashev, and Perel¹⁶ and Bobashev,¹⁷ and by Crothers.¹⁸ We consider Σ - Σ crossings such as those that occur near $b = 0.4$ a.u. and idealize them by straight lines as indicated in Fig. 10. For purposes of analysis we assume the amplitude for the $(1s\sigma 2p\sigma)^1\Sigma$ state is given by b_1^- while b_2^- denotes the $(1s\sigma 2s\sigma)^1\Sigma$ state. Rotational coupling to the $(1s\sigma 2p\pi)^1\Pi$ state is assumed to occur at $R = R_{\min}$.

In the original formulation of Ankudinov, Bobashev, and Perel¹⁶ and Bobashev,¹⁷ the amplitudes, at avoided adiabatic crossings, are related by

$$\begin{pmatrix} b_{II}^+ \\ b_I^+ \end{pmatrix} = \begin{pmatrix} S^* & -g^* \\ g & S \end{pmatrix} \begin{pmatrix} b_{II}^- \\ b_I^- \end{pmatrix}, \quad (3)$$

where b_{II}^- and b_I^- are the population amplitudes of adiabatic states Σ_2 and Σ_3 before the "curve crossing" and b_{II}^+ and b_I^+ are the population amplitudes after the crossing (see Fig. 11). The values of S and g are related to the physical characteristics of the avoided crossing:

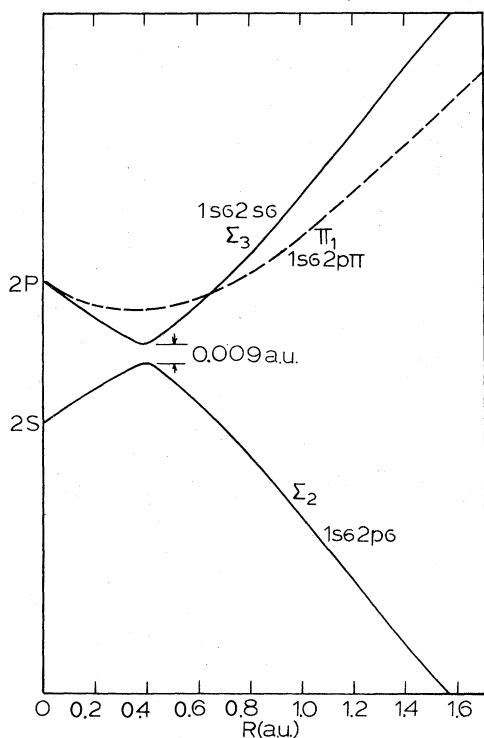


FIG. 10. Landau-Zener curve crossings for $2p\sigma$, $2s\sigma$, and $2p\pi$ states near united-atom limit.

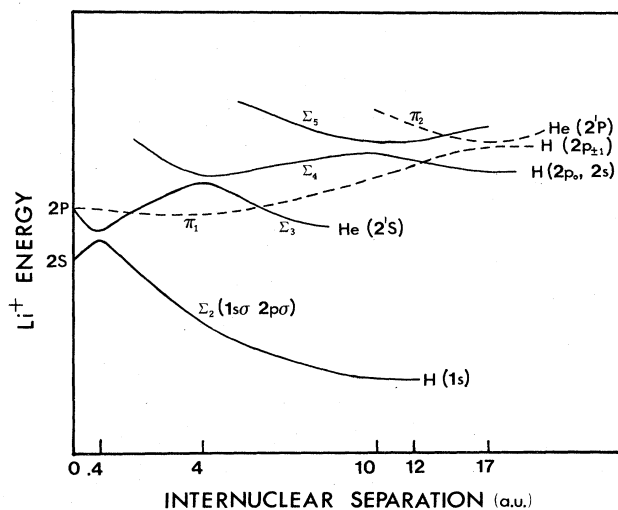


FIG. 11. Schematic diagram of curve crossings leading to final separated-atom states $\text{H}(2p) + \text{He}^+$.

$$S = \frac{\sqrt{2\pi\gamma}}{|\Gamma(1+i\gamma)|} \exp \left[-\frac{\pi\gamma}{2} + \frac{i\pi}{4} + i\gamma(\ln\gamma - 1) - i \arg[\Gamma(1+i\gamma)] \right], \quad (4)$$

$$g = g^* = \exp(-\pi\gamma), \quad (5)$$

where

$$\gamma = [(E_{II} - E_I)/2\hbar]_{R_x}^2 / [(H_{11} - H_{22})/\hbar(t - t_0)]. \quad (6)$$

Equation (3) can be applied to the physical situation illustrated in Fig. 10 or to any other region where the adiabatic curves exhibit isolated and avoided crossings. The phase change of the population amplitudes after traversing the avoided crossing is determined by the imaginary exponential factors in S ; $i \arg[\Gamma(1+i\gamma)]$, $i\pi/4$, and $i\gamma(\ln\gamma - 1)$.

Application of Eq. (3) to successive curve crossings gives the relationship between b_1^- , the population amplitude of the incoming $2p\sigma$ state, and b_1^+ and b_2^+ , the outgoing population amplitudes of the $2p\sigma$ and $2s\sigma$ states, respectively. Initially (see Fig. 10), all of the amplitude is in the $2p\sigma$ state, i.e., $b_1^- = 1$ and $b_2^- = 0$. The incoming amplitudes b_2 and b_1 in the region between R_0 and R_{\min} are then

$$\begin{pmatrix} b_2 \\ b_1 \end{pmatrix} = - \begin{pmatrix} S^* & -g^* \\ g & S \end{pmatrix} \begin{pmatrix} 0 \\ 1 \end{pmatrix} = \begin{pmatrix} g \\ -S \end{pmatrix}, \quad (7)$$

where the minus sign results from \dot{R} being negative on the "incoming" part of the interaction.

The population amplitude b_π of the $2p\pi$ state results from the rotational coupling, near R_{\min} , between $2s\sigma$ (adiabatic designation) and $2p\pi$ states. It is assumed that no phase change results from this transition. After rotational coupling occurs we have the amplitudes Ab_2 ,

$b_\pi = Bb_2$, and b_1 for the $2p\sigma$, $2p\pi$, and $2s\sigma$ states, subject to the condition $|A|^2 + |B|^2 = 1$. The values of A and B are chosen to be consistent with the 8-keV experimental data of Taulbjerg *et al.*¹⁵

Phase development arises from two distinguishable sources: an adiabatic phase factor $-(i/\hbar) \int_{t_0}^t E dt$ which develops in time due to the kinetic nature of the wave function; and ϕ_k , which is generated at the transition points where the potential curves cross.¹⁶ Thus the relative phase difference χ between the amplitudes of the states for $H(2p_0)$ and $H(2p_{\pm 1})$ can be written

$$\chi = \chi_\Pi - \chi_\Sigma = \left[- \int_{t_0}^{\infty} E_\Pi dt / \hbar + \phi'_\Pi \right] - \left[- \int_{t_0}^{\infty} E_\Sigma dt / \hbar + \phi'_\Sigma \right], \quad (8)$$

where the phase change resulting from a single crossing,

$$\phi_k = \frac{\pi}{4} + \gamma(\ln \gamma - 1) - \arg[\Gamma(1 + i\gamma)],$$

is from Eq. (4). The prime on ϕ'_k indicates it is the accumulated phase change from several crossings.

Transitions occurring at R_0 are described by

$$\begin{pmatrix} b_2^+ \\ b_1^+ \end{pmatrix} = \begin{pmatrix} S^* & -g^* \\ g & S \end{pmatrix} \begin{pmatrix} Ab_2 \\ b_1 \end{pmatrix} \\ = \begin{pmatrix} Ab_2 S^* - g^* b_1 \\ Agb_2 + b_1 \end{pmatrix} = \begin{pmatrix} Ag^* S^* + g^* S \\ Agg - SS \end{pmatrix}. \quad (9)$$

The amplitudes b_2^+ , b_1^+ , and b_π are then related to $H(2p_0, 2s)$, $H(1s)$, and $H(2p_{\pm 1})$ populations, respectively. If no further crossings were to occur $\sigma_1/\sigma_0 = |b_\pi|^2/|b_2^+|^2$ and χ is the relative phase between b_π and b_2^+ .

From the calculated potential curves of Green *et al.*,⁴ various γ 's were determined for the relevant crossings. For our experimental conditions, the relative phase due to internal ($R < 1$ a.u.) interactions is $< 10^\circ$. Further avoided crossings at larger R dominate the relative phase.

Further transitions at larger R occur at avoided cross-

ings shown schematically in Fig. 11. Application of Eq. (3) results in an overall calculated Π - Σ phase difference of $|45^\circ|$.

The agreement between this calculated phase and our measured value may be fortuitous because of the large number of crossings that must be taken into account. However, we do wish to point out that this is a mechanism for phase generation in collisions that is generally neglected and that it merits further investigation.

V. CONCLUSIONS

Perhaps a more promising approach to some understanding of inelastic mechanisms suggests itself in the sameness of the polarization patterns as shown in Fig. 3. Not only for the 4-keV patterns shown but for 5 and 8 keV as well, the general pattern is aligned at about the same angle relative to the beam. This suggests that one can interpret these data as resulting from a "freezing" of the electron cloud during some part of the collision that is approximately independent of impact parameter. Such a mechanism has been used to describe earlier impact-parameter-independent phase measurements of Jaecks *et al.*⁸ and Reiland *et al.*¹⁹

The work presented here invites a detailed calculation for comparison. The system is sufficiently simple that a good check with theory is possible. It is clear that translational coupling has as much an active part in the process as does rotational coupling. A detailed coupled-state calculation would be useful in determining the additional details apparent in the data. It is clear that the phase information in these calculations is an important aspect which cannot be ignored.

ACKNOWLEDGMENTS

The authors would like to thank Professor Joe Macek for the many informative and stimulating discussions regarding this experiment. We thank Dr. Tom Green for sharing the results of calculations on the HeH^+ system. This work was supported by the National Science Foundation.

*Present address: Department of Physics, Louisiana State University, Baton Rouge, Louisiana 70803.

¹D. H. Jaecks, A. Goldberger, M. Natarajan, N. Montgomery, and D. Mueller, in *Physics of Electronic and Atomic Collisions, Invited Papers of the XII International Conference, Gatlinburg, Tennessee, 1981*, edited by S. Datz (North-Holland, Amsterdam, 1982).

²U. Fano and W. Lichten, *Phys. Rev. Lett.* **23**, 157 (1969).

³K. Taulbjerg and J. S. Briggs, *J. Phys. B* **8**, 1895 (1975); F. J. Eriksen, D. H. Jaecks, W. deRijk, and J. Macek, *Phys. Rev. A* **10**, 2174 (1976).

⁴T. A. Green, H. H. Michels, J. C. Browne, and M. M. Madsen, *J. Chem. Phys.* **61**, 5186 (1974); T. A. Green, H. H. Michels, and J. C. Browne, *ibid.*, **64**, 3951 (1976).

⁵D. G. Crandall, R. H. McKnight, and D. H. Jaecks, *Phys. Rev. A* **7**, 1261 (1973).

⁶W. R. Ott, W. E. Kauppila, and W. L. Fite, *Phys. Rev. Lett.*

19, 1361 (1967).

⁷W. Reiland, G. Jamieson, U. Tittes, and I. V. Hertel, *Z. Phys. A* **307**, 51 (1982).

⁸D. H. Jaecks, F. J. Eriksen, W. deRijk, and J. Macek, *Phys. Rev. Lett.* **35**, 723 (1975).

⁹F. J. Eriksen, D. H. Jaecks, W. deRijk, and J. Macek, *Phys. Rev. A* **14**, 119 (1976).

¹⁰J. Macek and D. H. Jaecks, *Phys. Rev. A* **4**, 2288 (1971).

¹¹V. Dose, *Helv. Phys. Acta* **41**, 261 (1968).

¹²J. Fayeton, J. C. Houver, M. Barat, and F. Masnon-Seeuws, *J. Phys. B* **9**, 461 (1976).

¹³R. H. McKnight and D. H. Jaecks, *Phys. Rev. A* **4**, 2281 (1971).

¹⁴D. H. Crandall and D. H. Jaecks, *Phys. Rev. A* **4**, 2271 (1971).

¹⁵K. Taulbjerg, J. S. Briggs, and J. Vaaben, *J. Phys. B* **9**, 1351 (1976).

¹⁶V. A. Ankudinov, S. V. Bobashev, and V. I. Perel, *Zh. Eksp.*

- Teor. Fiz. **60**, 906 (1971) [Sov. Phys.—JETP **33**, 490 (1971)].
- ¹⁷S. V. Bobashev, *Invited Papers and Progress Reports of the Seventh International Conference on the Physics of Electronic and Atomic Collisions, Amsterdam, 1971*, edited by M. Barat (North-Holland, Amsterdam, 1972).
- ¹⁸D. S. F. Crothers, *Adv. At. Mol. Phys.* **17**, 55 (1981).
- ¹⁹W. Reiland, G. Jamieson, U. Tittes, and I. V. Hertel, *Z. Phys. A* **307**, 51 (1982).